AALBORG UNIVERSITY

DENMARK

AAU-DLR 2010 Indoor Measurement Campaign

Measurements for Validation of Models for Reverberant and Cooperative Channels

Steinböck, Gerhard; Pedersen, Troels; Wang, Wei

Link to publication from Aalborg University

**AAU-DLR 2010 Indoor
Measurement Campaign**

Measurements for Validation of Models for Reverberant and Cooperative Channels

Steinboeck G., Pedersen T., Wang W.

Version: 0.2   Date: 15.06.2011

CONTENTS

CHAPTER 1

MOTIVATION AND PURPOSE FOR THE MEASUREMENT CAMPAIGN

The measurement campaign has two main motivations. One motivation is to provide measurement data to validate models for in-room channel models including reverberation effects and the other motivation is to provide measurement data for cooperative localization methods.

1.1 Motivation for Validation of In-room Reverberant Model

A path loss model was developed based on observations of the behavior of the delay power spectrum. Previous measurement campaigns e.g. in the WHERE project, are not fully suitable for validation due a limited amount of data in the spatial domain. For the validation of the proposed model it is necessary to have transmitter receiver distances covering almost all possible distances in the room. Furthermore the data should allow for spatial averaging at the transmitter and receiver side in order to minimize the influence of small scale fading on the path loss.

One further motivation is to use the experimental data to find out or confirm the physical reasoning for the observed reverberation behavior. The data should also allow for the development of further models accounting for reverberation phenomena.

1.2 Motivation for the Cooperative Localization Measurements

There is to our knowledge no measurement data for cooperative localization available. We have defined scenarios that cover a. LoS and b. NLoS links between
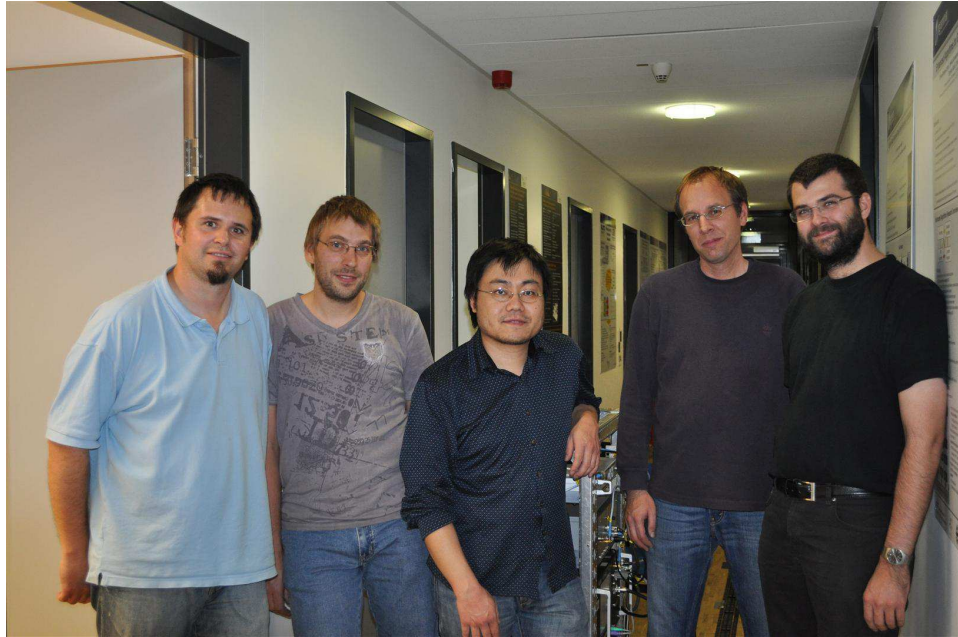
Figure 1.1: Measurement team. (From left to right: Steinboeck G., Jost T., Wang W., Raulefs R. and Pedersen T.)

transmitter and receiver. The three tracks of the train cover potential positions from three sides. This offers a robust approach for distance-based evaluations.

1.3   Measurement Team

The measurements were conducted in cooperation between the Institute for Communication and Navigation from German Aerospace Center (DLR) and the Navigation and Communication Section of Aalborg University (AAU). The people involved during the planing phase of the measurements were Ronald Raulefs and Wei Wang from DLR and Bernard Fleury, Troels Pedersen, and Gerhard Steinboeck from AAU.

During the measurement campaign the main actors were Thomas Jost, Ronald Raulefs, and Wei Wang from DLR. From AAU Troels Pedersen and Gerhard Steinboeck participated in the measurements. The team was supported by numerous other people during measurements, e.g. people taking photos or participating in the experiment described in Section 5.2.3. The measurement team is shown in Fig. 1.1.

CHAPTER 2

ENVIRONMENT

2.1 Measurement Environment

We consider an office environment at DLR premises. A floor plan is shown in Fig. 2.1. The building has 3 story heights above ground floor and a basement. The rooms considered are on the ground floor. The main focus was on the meeting room indicated as R4, because it was the largest room available. Fig. 2.2 shows the meeting room R4, and two offices R3 and R2. At a room height of 2.78 m is a intermediate ceiling of approx. 2 cm hard "mineral wool" slabs . The mineral wool slabs are mounted with metal frames to concrete ceiling with approximately 30 cm distance. The floor was wooden with concrete underneath. The outer walls mainly consist of windows with metallic coating occasionally interrupted by concrete pillars. The inner walls are drywalls and are the same for all inner walls. There are white boards in each room with the size of $1.8 \times 1.2 \text{m}^2$.

The transmitting antenna was mounted for the measurements on a model train at a height of 1.26 m. We considered two tracks of the model train in the meeting room R4, indicated with T1 and T2 and one track in in the office R3 labeled as T3.

The circular receiver antenna array with 8 elements was placed on several positions in the three rooms marked with red crosses. The receiver positions labeled with Rp1 to Rp9 are measured from all tracks and are at a height of 1.1 m. For the cooperative localization 10 additional receiver positions labeled as T1Rp1 to T1Rp5 and T2Rp1 to T2Rp5 at a height of 1.2 m were added. The channel was measured for these positions only with track T3 and T1 or T2 respectively.

Doors and windows are closed during the measurements, otherwise indicated.

The positions of white boards, heaters, windows, pillars, table, the receiver coordinates and several other things with respect to the walls have been measured as well. The results are indicated in Fig. 2.4.

The distance to the tree line outside of the building (see e.g. Fig. 4.2 in the windows) is approximately 22 m.
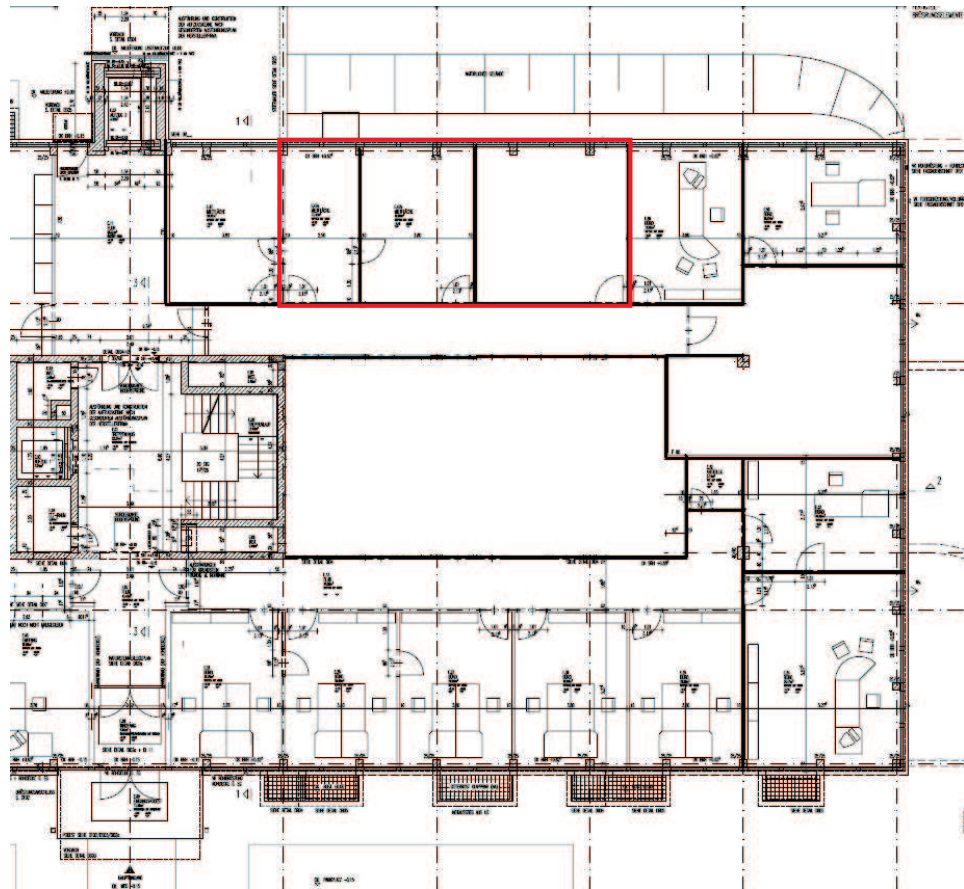
Figure 2.1: Ground floor of the DLR building. The red rectangle outlines rooms R2, R3 and R4 considered in the measurement campaign.
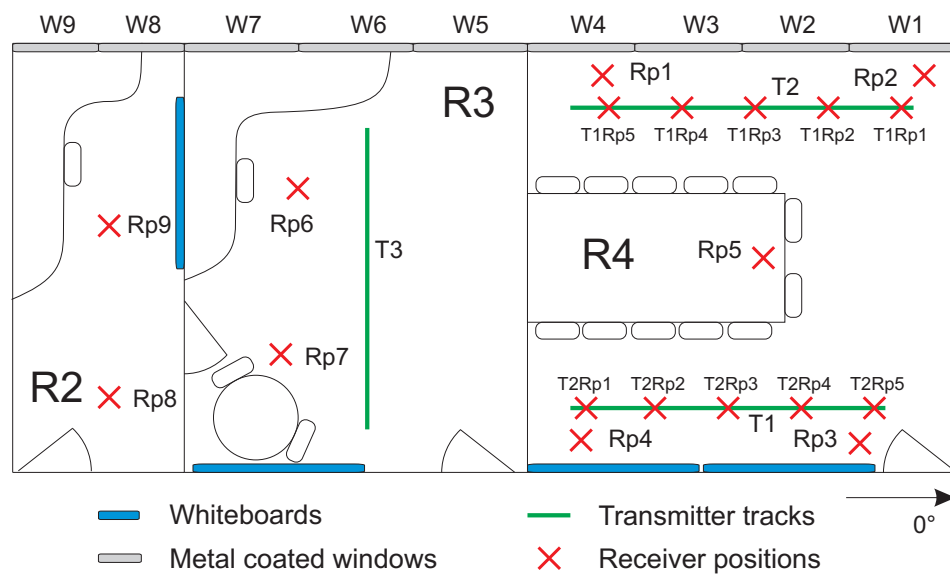
Figure 2.2: DLR premises for the measurement campaign.

2.2 Measuring Distances

The receiver and transmitter positions have been measured with a tachymeter and the coordinates are available in different formats. The moving of the transmitter was recorded with the tachymeter. In addition during the measurements were odometer pulses recorded with the channel sounder receiver unit.

The model railway is running on a cogwheel to prevent wheel slipping. The HEDL 5540 rotary encoder mounted on the model train engine counts the engine turns by giving 500 impulses per full rotation. This allows determining the odometer factor defined as the number of impulses per meter from measurements. To obtain this value, $K = 21$ train runs have been performed with traveled distance m_k and counted encoder impulses n_k for each run $k = 1, ..., K$. The odometer factor ρ is calculated as the sample mean

$$\rho = \frac{1}{K} \sum_{k=1}^{K} \frac{n_k}{m_k} . \tag{2.1}$$

Based on the K measurements, ρ is determined as $105212.52 \, \mathrm{m}^{-1}$. It indicates that the rotary encoder counts around 105212 impulses per traveled meter. This translates into $\simeq 105$ impulses for a traveled distance of $1 \, \mathrm{mm}$. In general a rotary encoder with less impulses per motor turn might be used, with the drawback of less spatial resolution. An estimate $\hat{m}$ of the traveled distance can be calculated straightforward as

$$\hat{m}_k = \frac{n_k}{\rho} . \tag{2.2}$$

The estimation error ζ_k between $\hat{m}_k$ and the true distance m_k normalized to m_k is defined as

$$\zeta_k = \frac{\hat{m}_k - m_k}{m_k} . \tag{2.3}$$

Taking all K measurements into account a mean error $\mu = -0.0024 \, \mathrm{mm/m}$ with standard deviation $\sigma = 0.2266 \, \mathrm{mm/m}$ is obtained as shown in Fig. 2.3. By storing the number of rotary encoder impulses synchronously with each measured CIR snapshot, since the start of the train movement, a traveled distance for each CIR snapshot can be obtained in a straightforward manner.

Unfortunately, the channel sounder raw data file format provides not the recorded number of odometer pulses. Instead a distance value with the configured number of pulses per meter is stored. The channel sounder has a limitation on the number of odometer pulses (100000) per meter. Thus one can calculate the corrected moved distance d_{true} along the track since the start of a measurement run as:

$$d_{true} = \frac{I_{Nav}}{I_{real}} \cdot d_{Nav}, \tag{2.4}$$

where I_{Nav} was set to the maximum possible number of odometer pulses (100000) in the channel sounder, I_{real} corresponds to above obtained $\rho = 105212$ and d_{Nav} is the distance recorded in the measurement data. The values of d_{Nav} and I_{Nav} can be retrieved from the raw data files using the Matlab function RSKNav from MEDAV.
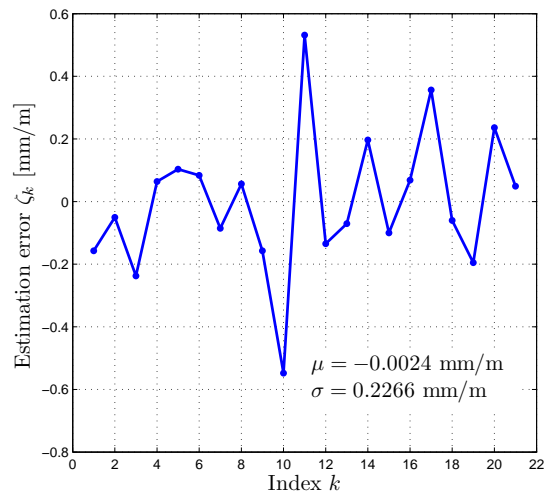
Figure 2.3: Estimation error of the distance for the $K = 21$ measurements obtained with $\rho = 105212$.
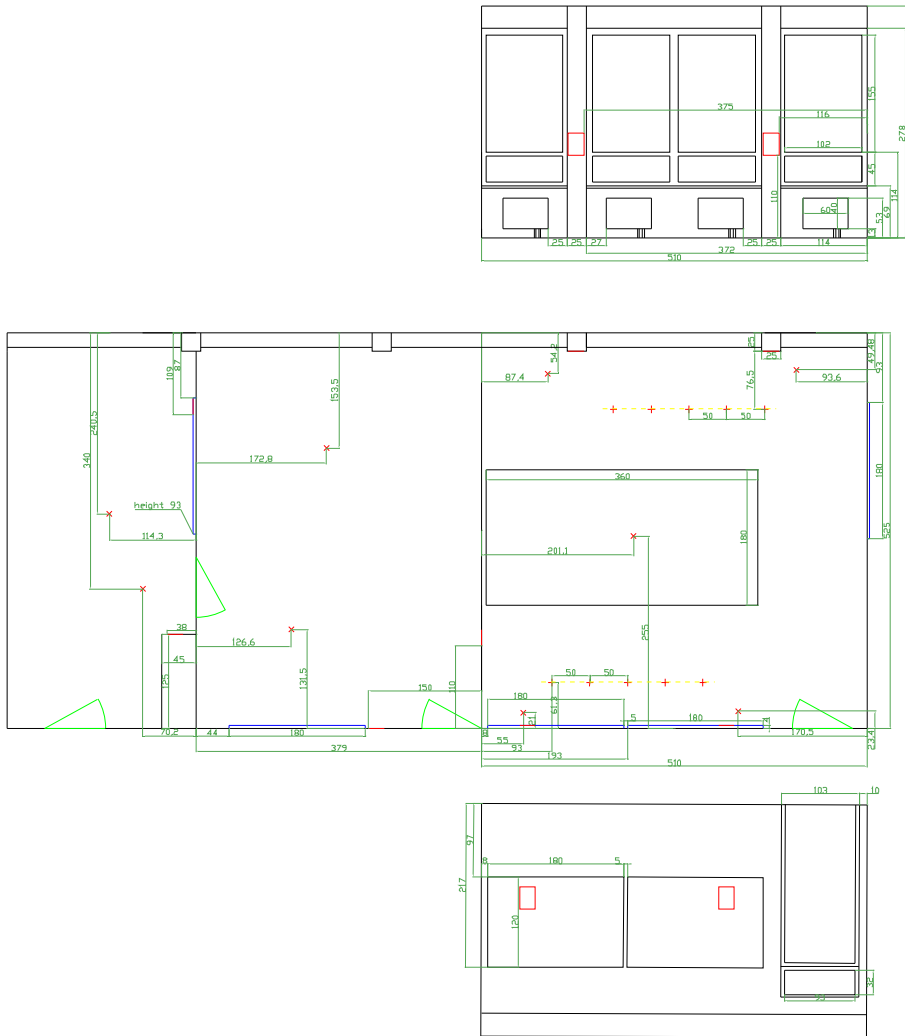
Figure 2.4: Measurements of the environment taken during the measurement campaign.

CHAPTER 3

CHANNEL SOUNDING EQUIPMENT

3.1 Channel Sounder and Setup

In the diagram of Fig. 3.1 is the general measurement setup shown. The three channel sounder units (transmitter, receiver and clock generator) were placed outside of room R4 in the corridor. The transmitter antenna was placed on a model train moving along T1, T2, or T3. During movement the train odometer creates pulses which are recorded from the receiver unit and stored together with the measurement data. The receiver unit of the channel sounder controls the multiplexer of the receive antennas.

3.1.1 Synchronization of Transmitter and Receiver

The transmitter and the receiver were both connected via same type of coaxial cables of length approximately 60 m with the rubidium clock generator unit of the channel sounder.

3.1.2 Transmitter Measurement Setup

The transmitter setup is shown in Fig. 3.1. The transmit antenna is mounted on a rail road car of a model train is shown in Fig. 3.8b. The height of the transmit antenna is 1.26 m.

3.1.3 Receiver Measurement Setup

The antennas were connected with short cables to the inputs of the multiplexer (see e.g. Fig. 3.2). The output of the multiplexer was connected with a 9 m long low-loss RF-cable SUCOFLEX 100 from Huber&Suhner with attenuation of 6 dB, labeled as "Z10A" to a 10 dB attenuator (R1) which was directly connected to the input of the low noise amplifier (LNA). The LNA has a gain of 50 dB. The
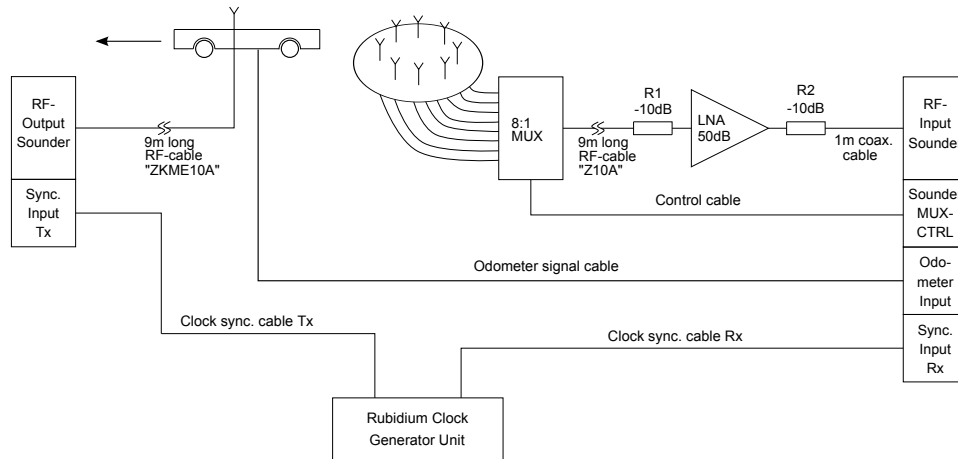
Figure 3.1: Overview of the measurement setup for Tx and Rx.
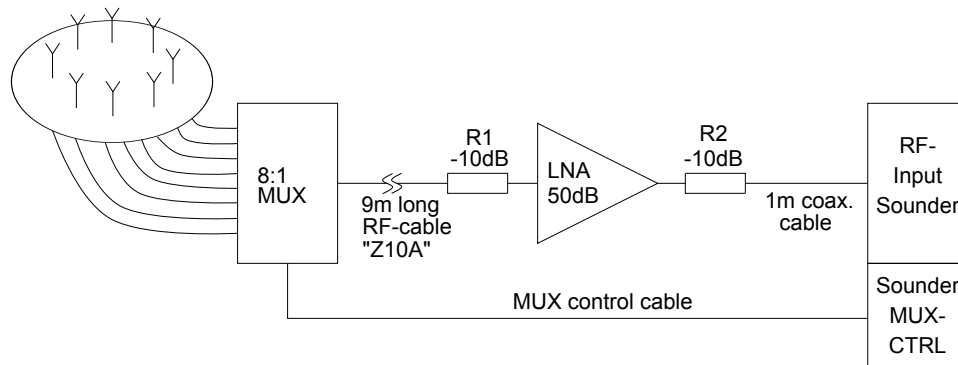
Figure 3.2: Receiver measurement setup.

noise figure of the LNA is about 1.5 dB and the effective bandwidth of the LNA is 120 MHz. The attenuator R1 from Rohde & Schwarz was used to prevent saturation of the LNA input for very short distances between transmitter and receiver. Directly on the output of the LNA was the attenuator R2 similar as R1 from Rohde & Schwarz (10 dB) connected to prevent saturating the RF input of the channel sounder. From R2 a short coaxial cable (1 m) was used to connect to the receiver input of the channel sounder. The attenuator R1 was removed for measurements when the Tx and Rx were separated in different rooms in order to keep a high SNR for those measurements.

3.1.4   Receive Antenna Array and Multiplexer

In Fig. 3.3 is the topview of the receiver array shown. The zero direction of the array is from the center towards antenna 1. The center of the array is the coordinate system. The antennas are equidistantly spaced ($45°$) on a circle with diameter of 75.18 mm. The receiver antenna 1 was connected to multiplexer port 1, antenna 2 to port 2, and so forth for all antennas. The cable connections from the antenna array to the multiplexer are shown in Fig. 3.4c. A laser pointer was mounted on
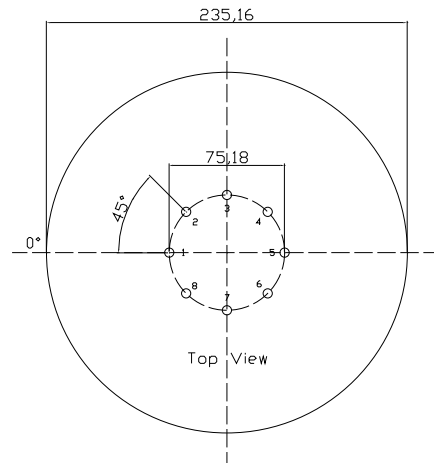
Figure 3.3: Rx antenna array topview. The $0°$ symbol in the drawing marks the $0°$ direction of the antenna array.

the array pointing into the $0°$ direction. This laser pointer was used in order to rotate the array such that the $0°$ direction is parallel to the wall along the corridor (opposite of the windows) as indicated in Fig. 2.2. The antenna array and the multiplexer were mounted on a tripod. A height of either 1.1 m or 1.2 m to the upper edge of the ground plane was used during the measurements.

The utilized time division multiplexer was manufactured by VAD GmbH in Dresden, Germany. This multiplexer contains a 8-of-1 pin diode switch with impedance matching inputs. In other words, if one antenna (channel) is switched on, thus connected to the out gate, the other seven antennas (channels) are closed and loaded with 50 Ω. The matched impedance at off-channels with 50 Ω ensures that there are no reflections from these antennas. A validation test on the multiplexer in the lab at DLR confirms the specifications of the multiplexer datasheet described above.

Antenna Array Calibration

Generally, if the array's position is known, with a sufficient amount of measured steering vectors, it is possible to identify the antenna calibration matrix and multiplicative constants by solving the nonlinear least squares problem.

The calibration for the antenna array is performed in a free space like environment at DLR. Referred to the carrier frequency, a narrow band signal was transmitted through a non-reflecting propagation channel. This means only one LoS path is expected during the calibration measurement. The environment ensures far field waves impinging on the antenna array, and mainly only one line of sight component exits. The transmit antenna and receive antenna were approximately 20 mseparated from each other.

Fig. 3.5 gives the definition of the incoming angles utilized in the calibration measurement. The arrow in the plot represents the impinging wave, and the corresponding azimuth angle α and elevation angle β definitions for the provided coordinate system are depicted. During the calibration measurement, the antenna array

(a)

(b)

(c)

Multiplexer

(d)
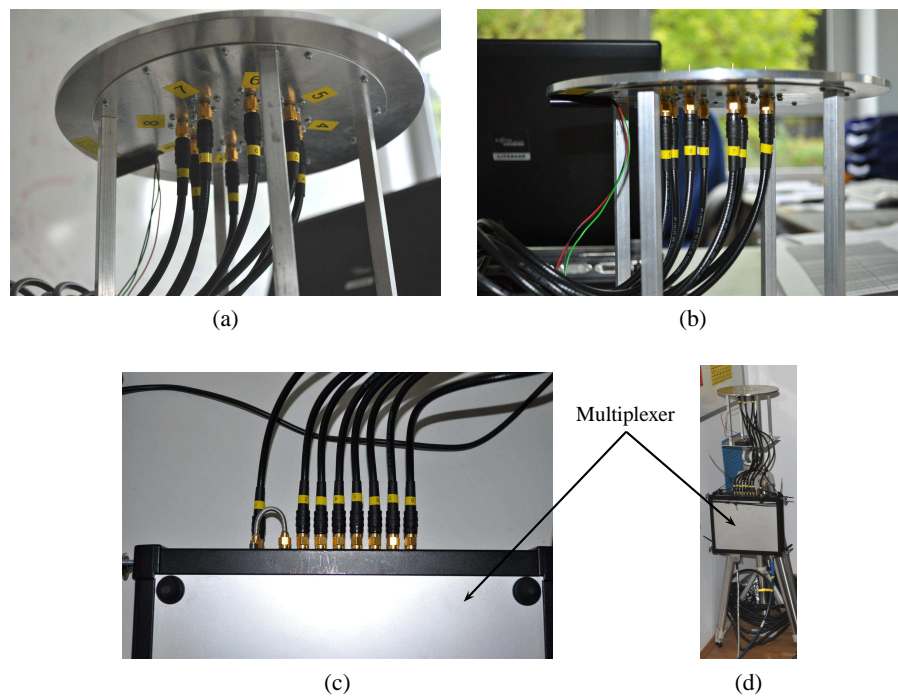
Figure 3.4: (a) connection of the cables and the antennas shown from the bottom of the array; (b) view from the side of the array and cables; subref-fig:switchrxantcables connection of the cables to the multiplexer; (d) to the left, the multiplexer and receiver antenna array on the tripod - to the right the model train with the transmit tower.
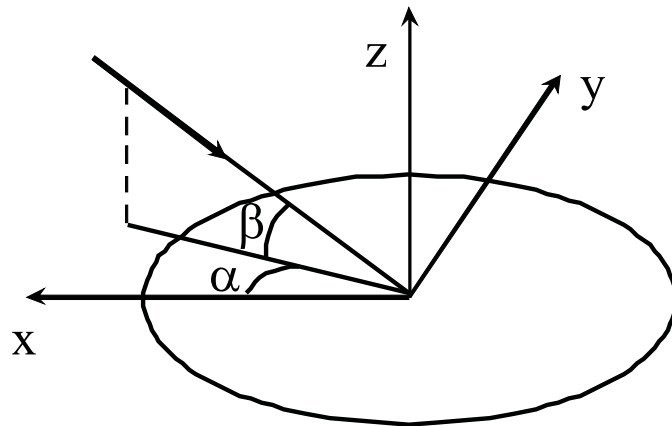
Figure 3.5: Definition of the incoming angles.
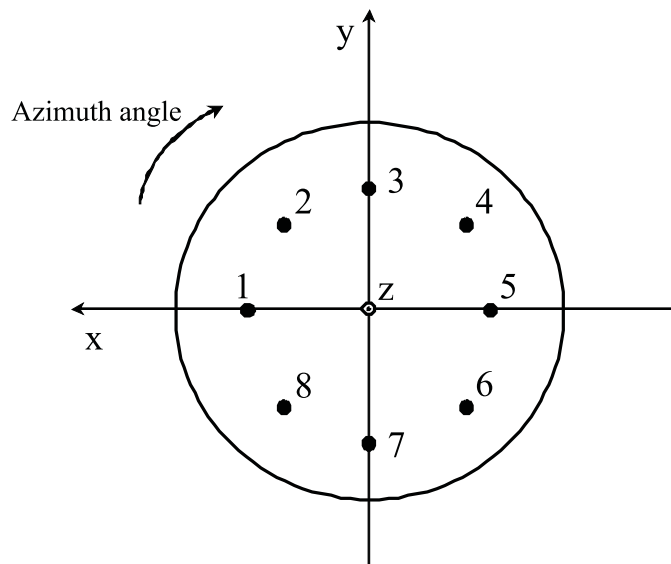
Figure 3.6: Rotation of antenna array to change the incoming azimuth angle.

was rotated in vertical plane with 5° steps to change the incoming azimuth angle. The array was rotated in the horizontal plan in 5° steps to change the incoming elevation angle as shown in Fig. 3.6 and Fig. 3.7. The azimuth angle was taken from 0 to 355°. For each azimuth angle, the antenna array was rotated in elevation from 0 to 90°.

3.1.5 Transmit Antenna

Transmit antenna: Huber&Suhner Type SOA 5600/360/3/20/V_1 [1] mounted on a circular groundplane of diameter 235.16 mm. The antenna was mounted on the tower of the model train at a height of 1.26 m measured from the floor to the upper edge of the groundplane.
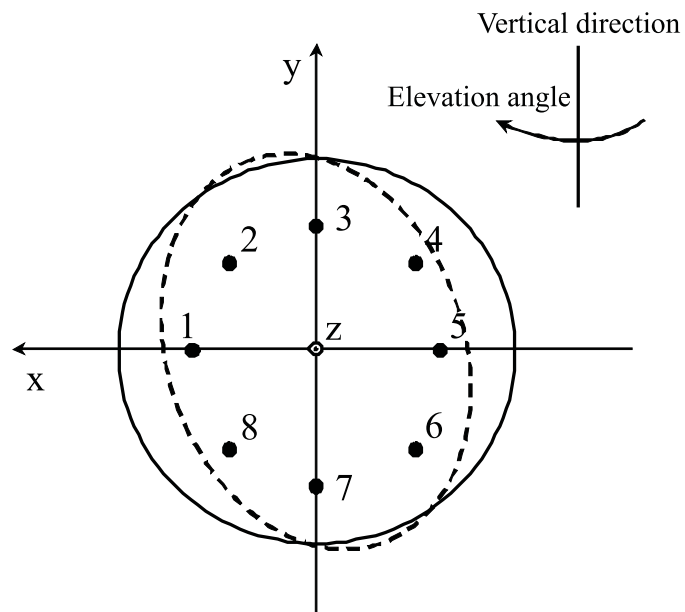
Figure 3.7: Rotation of antenna array to change the incoming elevation angle.

(a)   (b)
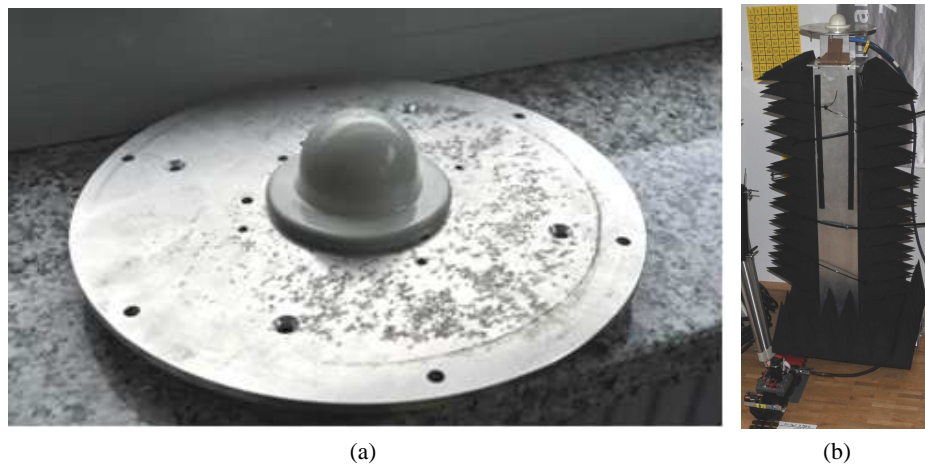
Figure 3.8: (a) shows the Hubner&Suhner transmit antenna mounted on the groundplane disc. (b) shows the transmit antenna mounted on the tower of the model train at the height of 1.26 metre.

3.2 Sounder Settings

In Table 3.2 are the used sounder settings summarized.

3.2.1 Sounding Signal

The duration of the sounding signal is $T_{\mathrm{Tx}} = 12.8\,\mu s$. The measurement bandwidth is 120 MHz, with $N_c = 1536$ frequency tones. The inter-tone spacing is 78.125kHz.

3.2.2 Sounding Mode

The sounder was operating in the Fast Doppler (FD) and time grid mode. The timing scheme of the sounder is shown in Fig. 3.9.

The duration of the sounding pulse is denoted by T_{Tx}. The multiplexer sequentially switches the N_{Rx} elements of the receive antenna array. For each element measured, two sounding pulses are transmitted, thus the time duration T_{Rx} between the start of the measurement of two antenna elements is

$$T_{\mathrm{Rx}} = 2 \cdot T_{\mathrm{Tx}} \tag{3.1}$$

The time duration of a measurement cycle in which all receive antennas are measured once, is

$$T_{\mathrm{cycle}} = N_{\mathrm{Rx}} \cdot T_{\mathrm{Rx}} = 2N_{\mathrm{Rx}}T_{\mathrm{Tx}} \tag{3.2}$$

In "Fast Doppler mode" the sounder measures a "burst" of N_{burst} cycles consecutively. The duration of one burst is

$$T_{\mathrm{burst}} = N_{\mathrm{burst}} \cdot T_{\mathrm{cycle}} = 2N_{Rx}N_{\mathrm{burst}}T_{\mathrm{Tx}} \tag{3.3}$$

After each burst the sounder stores the recorded data and a break is for data storage is inserted. After the data is stored, the next burst is measured. Thus the time interval between consecutive bursts are

$$T_{\mathrm{rep}} = N_{\mathrm{rep}}T_{\mathrm{burst}} \tag{3.4}$$
$$= 2N_{\mathrm{Rx}}N_{\mathrm{burst}}N_{\mathrm{rep}}T_{\mathrm{Tx}} \tag{3.5}$$

for some constant N_{rep} which is calculated by the sounder based on its hardware constraints.

Let the data acquired during one sensing period of a single antenna element be called a sub-channel sample. Then the ith sample is acquired at center time

$$t_i = (i-1 \quad \mathrm{mod}\ N_{\mathrm{Rx}}N_{\mathrm{burst}})T_{\mathrm{Rx}} + \left\lfloor \frac{i}{N_{\mathrm{Rx}}N_{\mathrm{burst}}} \right\rfloor T_{\mathrm{rep}}, \qquad i = 1,2,3,\ldots \tag{3.6}$$

The ith sample is acquired from the antenna element with index

$$m(i) = i \quad \mathrm{mod}\ N_{\mathrm{Rx}}, \qquad i = 1,2,3,\ldots \tag{3.7}$$

During one burst, the transmitter moves

$$d_{\mathrm{burst}} = v_{\mathrm{Tx}}T_{\mathrm{burst}} \approx 0.0035\lambda, \tag{3.8}$$

and in between each burst it moves

$$d_{\mathrm{rep}} = v_{\mathrm{Tx}}T_{\mathrm{rep}} \approx \frac{\lambda}{8.8}. \tag{3.9}$$

Table 3.1: Timing Scheme Settings

Parameter	Symbol	Value
Number of receive antennas	N_{Rx}	8
Number of cycles per burst	N_{burst}	20
Number of bursts in the burst repetition time	N_{rep}	32
Transmit pulse length	T_{Tx}	12.8 µs
Interval between consecutive Rx measurements	$T_{Rx} = 2T_{Tx}$	25.6 µs
Burst duration	$T_{cycle} = 16T_{Tx}$	204.8 µs
Burst duration	$T_{burst} = 320T_{Tx}$	4 096 µs
Burst repetition time	$T_{rep} = 10240T_{Tx}$	131.072 ms
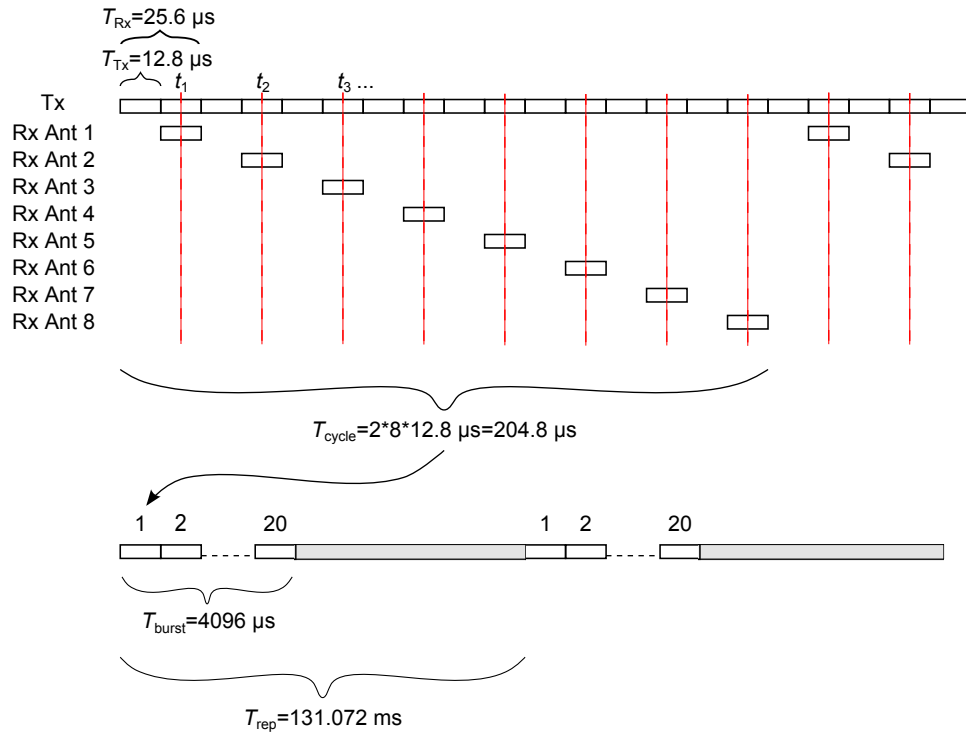
Figure 3.9: Timing schema used for the measurements.

Table 3.2: Setting of the channel sounder.

Parameter	Value
Carrier frequency f_c [GHz]	5.2
Bandwidth B [MHz]	120
Number of sub-carriers N_c	1536
Carrier separation Δf [kHz]	78.125
Tx velocity [m/s]	≈ 0.05
Odometer pulse correction I_{real}	105212.523942

CHAPTER 4

RECORDING OF SPHERICAL PANOGRAPHS

During the preparation time panographs were made (full 360° in azimuth and full 180° in co-elevation) for all receiver positions at the height of the Rx antennas. The panographs show the whole scene viewed from each of the receiver positions. This allows for overlaying direction estimates on the photos.

One way of creating panographs with $360° \times 180°$ is to use multiple rows and columns of photos to "stitch" one big panograph. The photos should overlap and should have enough features in the overlapping area to align the images in an automatic stitching process. For the purpose of creating a minimal number of images, a very short focal length, resulting in large viewing angles is preferred. We used the website [2] to get the viewing angle for the used focal length and the size of the image sensor of the camera. The viewing angles allow to calculate the number of images needed for the $360° \times 180°$ panograph.

4.1   Equipment and Stitching Software

For the purpose of creating panoramic images, specifically indoors where objects are very close, it is important to align the cameras "nodal" point precisely to the center of rotation. This is important in order to have near and far objects aligned in different images taken from different viewing angles. In case of misalignment ghostly artifacts of the object can appear on different positions in the panograph and the stitching process can fail. Note, in case the focal length on the camera is changed, the nodal point changes too.

In order to mount the camera in its nodal point and to rotate the camera correctly in azimuth and elevation, we used the panorama system VR-System 6/8 from Novoflex (see Fig. 4.1). To find the nodal point of the camera system and to adjust it correctly with the panorama system, we used the method described [3].

The used camera is a Nikon D5000 with a crop factor of 1.5 (image sensor size 15.8×23.6 m^2). The camera was equipped with a AF-S DX Nikkor 18-55 mm

1:3,5-5,6G VR lens system. The focal length of the lens system was set to 18 mm. The resulting field of view is in portrait orientation $47.4° \times 66.7°$. We chose a 30° step size in azimuth leading to 40% overlap of the images. In elevation we chose to take 5 rows in total. One row in the azimuth plane (0°elevation) and four rows with ±30° elevation and ±60° resulting in approximately 50% overlap.

For the stitching process we used the software "Stitcher Unlimited 2009" from Autodesk. The software allows for the creation of $360° \times 180°$ panographs from multiple rows and columns of images. The software supports multiple output formats. One of the formats creates a panograph with a equi-rectangular coordinate system for azimuth and elevation angles. This allows for easy mapping of e.g. directional Bartlett-spectra on the panograph.

4.2   Calibration and Use of Panographs

For calibration purpose and for stitching purpose colored posters were used. All posters show a numbered grid to assist in the stitching process. The right lower corner of the red posters is used for reference purposes. This corner is at the height of the receive antenna. Furthermore the distances in the room to the right lower corner of the red posters were measured. This allows to calculate reference angels from the receiver position to these posters. In addition known objects or other features (corners) of the room can be used to calculate reference angles. This allows to easily find the 0° direction (azimuth and elevation) in the panographs. The stitching software automatically adjusts the elevation angle to zero degree. This angle can be refined with the reference corner of the red posters, if necessary. The 0° azimuth is coarsely adjusted with the stitching software based on the known 0° direction such that the center of the image corresponds to 0° in azimuth and elevation.

After this adjustment in the stitching software we export the panograph in an equi-rectangular coordinate system for azimuth and elevation.

The size of the panograph in pixels corresponds to an image with ±180° in azimuth and ±90° in elevation. When importing the image into Matlab we map the image size in pixels to a coordinate system in degrees. A refinement of the 0° azimuth direction using the reference points is done by simple shifts of the image. The resulting calibrated images are stored for later use in Matlab with the 0° direction in the center of the image. The filenames of the calibrated images for the use in Matlab are listed in Table 4.1. An example image is shown in Fig. 4.2.

Figure 4.1: The panorama system VR-System 6/8 mounted on the tripod in (a) and with the camera in (b),(c), and (d). In (d) the setting of the focal length can be seen.
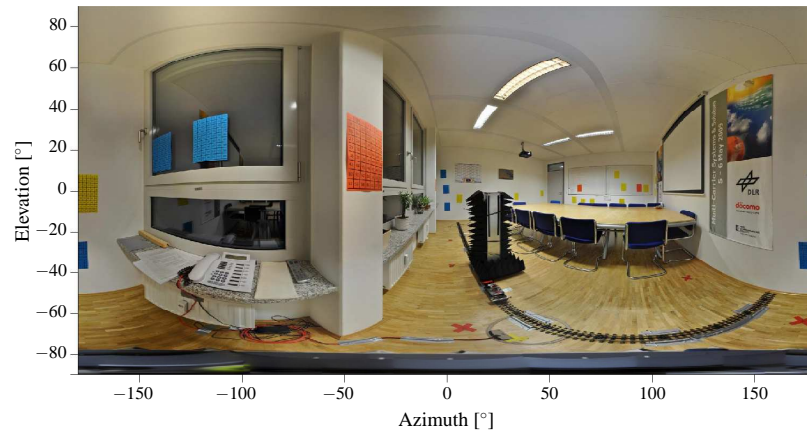
Figure 4.2: Spherical panoramic photo from Rp1 perspective. A equi-rectangular coordinate system for azimuth and elevation is used. The center of the image corresponds to $0°$ in azimuth and elevation.

Table 4.1: Panograph file names.

Receiver Position	Coarse adjustment with high resolution	Calibrated file for Matlab usage
Rp1	rp1_highres.jpg	rp1_matlab.jpg
Rp2	rp2_highres.jpg	rp2_matlab.jpg
Rp3	rp3_highres.jpg	rp3_matlab.jpg
Rp4	rp4_highres.jpg	rp4_matlab.jpg
Rp5	rp5_highres.jpg	rp5_matlab.jpg
Rp6	rp6_highres.jpg	rp6_matlab.jpg
Rp7	rp7_highres.jpg	rp7_matlab.jpg
Rp8	rp8_highres.jpg	rp8_matlab.jpg
Rp9	rp9_highres.jpg	rp9_matlab.jpg

CHAPTER 5

EXPERIMENTS

5.1 Experiments for Validation of In-room Path loss Model

The purpose of these measurements is the evaluation of the in-room reverberant channel model. For this evaluation it is necessary to have measurements with distances between Tx and Rx ranging from the smallest possible distance to the largest distance possible in the room. Thus the Rx is positioned in the room corners and the tracks for the Tx pass closely by the Rx. By choosing at the Rx a circular antenna array and placing the Tx on the model train, spatial averaging is possible for the evaluation of the path loss model. Furthermore the use of the circular array allows the creation of virtual Rx antenna patterns in order to evaluate the differences for localization with different virtual Rx antenna orientations.

5.1.1 Experiment 1.1: Noise Measurement

This experiment consists of a short measurement where the Tx is switched off and only "noise" at the receiver is measured. This should provide information on any present interference from e.g. the WiFi networks and allows to estimate the noise level. This obtained noise level might be different from the one later during the measurements due to the maximum dynamic range of the system.

5.1.2 Experiment 1.2: Path loss measurements for Rp1 to Rp9

For each of the indicated receiver position Rp1 to Rp9 are measurements conducted when the model train (transmitter) moves along the tracks T1 and T2. No people are in R4. People are working in R2 and R3. The used Tx tower height is 1.3 m.

5.1.3 Experiment 1.3: Static Measurements

Four static measurements for the receiver position Rp4 are conducted. The four positions of the transmitter are the start and end points of track T1 and track T2.

These measurements are control measurements to see if the environment can be considered static.

5.2   Reverberation Effect Experiments

In this experiment we conduct measurements with open windows or people present in the room. The windows are metal coated and when they are opened we expect a different reverberation in the room. By opening the windows we alter one wall of the room from low "absorption" (strong reflections from the windows) to high "absorption" coefficients (no reflections from the open window). Thus a lower power level for the reverberant field is expected.

The inner-walls of the building are drywalls and their attenuation (absorption) is unknown. It is unclear if the observed reverberation effect in the meeting room is generated by the room itself or by the larger structure of the building. If a change in the reverberation due to opening the windows in the neighboring rooms is observed, we conclude that the larger structure of the building creates the reverberation effect.

The underlying idea of the reverberation is based on reflections in the room with an average absorption coefficient. By adding persons to the room, the average absorption coefficient should change, thus the reverberation effect should change. We make the hypothesis that this alters the reverberant field in the room.

5.2.1   Experiment 2.1: Open Windows in Room R4

We use for the measurements track T1 for the transmitter. The receiver locations are Rp1 to Rp4. We conduct multiple measurements with different number of open windows until all windows in the room are open.

5.2.2   Experiment 2.2: Open Windows in Room R2 to R4

All windows in rooms R2, R3 and R4 are opened and we conduct measurements for the receiver locations Rp2 to Rp4 and the transmitter moving along track T1.

5.2.3   Experiment 2.3: Absorption of Human Bodies in the Room

Measurements are conducted with people in the meeting room sitting around the conference table. The receiver positions Rp2 to Rp4 are used for tracks T1.

5.3   Cooperative Localization Experiments

The purpose of these measurements is to provide measurement data for analyzing the multi-link radio channel for localization purposes. In room R4 the measurements are conducted for line of sight situations. Additional measurements from the neighboring rooms R2 and R3, corresponding to non-line of sight situations, are conducted as well.

5.3.1   Experiment 3.1: Cooperative Localization

Los Multi-link Measurements: Room R4 covers a scenario with only cooperative LoS links. We use the train track T1 with Rp1 and Rp2 and vice versa T2

with Rp3 and Rp4 from the experiment described in Section 5.1.2. This set is extended by five additional points on the opposing track. The train track T[1,2] and the T[1,2]_P[1..5] points were all measured with the same antenna height. With this we can investigate a mirroring effect as both measurements have the same conditions with the same sampling distances on both sides. The measurements for the points Rp[1..5] provide the possibilities to use a set of reference points for modeling anchors with perfect position information.

NLoS Multi-link Measurements: In room R3 a 3rd track and two more additional reference points (Rp6 and Rp7) are added. The 3rd track T3 allows to measure NLoS effects for the cooperative links established in room R4 together with a robust approach by using distance-based measurements. The robust approach is guaranteed as the geometrical constellation of the tracks (T3 vs. T[1,2]) is orthogonal to each other. The additional reference points Rp6 and Rp7 have LoS conditions to the track T3 to differ between having only LoS (R3) and NLoS (R4). This is further extended to room R2 and the points Rp8 and Rp9. The link between track T3 and Rp8 can be considered as strong NLoS (weak LoS) case, as the material in between transmitter and receiver is not concrete. The link between track T3 and Rp9 is blocked by a metallic white board and thus a weak NLoS link is expected.

5.4 Fluorescent Tube Experiment

5.4.1 Experiment 4.1: Fluorescent Tube

In previous measurement campaigns was reported that switched on fluorescent tubes create a time varying channel. An experiment at fixed transmitter and receiver positions is conducted to test this phenomenon in the given environment. The continuous radio channel is measured. In the few first seconds of the measurements, the fluorescent tubes are switched off and after a couple seconds the fluorescent tubes are switched on.

5.5 Measurement Protocol

In the following we summarize the measurement process and note exceptions which happened during the experiments. We refer the reader to Fig. 2.2, which shows a schematic of the measurement environment and to Fig. 4.2 showing a spherical panorama image from Rp1. The measurements are identified as scenarios numbered from 0.00 to 6.03, for practical reasons. Scenarios can be part of multiple experiments. A mapping of the scenarios to the corresponding experiments can be found in Table 5.1.

5.5.1 Measurement of Noise (Experiment 1.1)

A measurement of the noise was conducted before the measurements of the different scenarios were done. The measurement was conducted with the receiver at Rp4

and with the transmitter at the start position of T1. The main goal of this measure-
ment was to see the input on the receiver when the transmitter is turned off. This
should help to identify if there are any WiFi networks transmitting and if there are
any other disturbing sources in the measured band width. Furthermore it should
provide an indication of the noise power. Before this measurement was recorded,
a detailed check of the noise power, the signal power and the AGC settings was
done. Adjustments such as adding the LNA and tests with different attenuators
were conducted to optimize for the full range of the AGC and to achieve as much
SNR over all transmitter and receiver positions as possible.

Table 5.1: Mapping of Scenarios to Experiments.

Scen. #	Filename	Exp. 1.1: Noise	Exp. 1.2: Path loss	Exp. 1.3: Static	Exp. 2.1: Open windows in R4	Exp. 2.1: Open windows in R2 to R4	Exp. 2.1: Human absorption	Exp. 3.1: Coop. localization	Exp. 4.1: Fluorescent tubes
0.00	AAUDLR2010_noise_01	x							
1.01	AAUDLR2010_01_01_T1_Rp1		x	x					
⋮	⋮		⋮	⋮					
1.09	AAUDLR2010_01_09_T1_Rp9		x	x					
1.10	AAUDLR2010_01_10_T1_T2p1							x	
⋮	⋮							⋮	
1.14	AAUDLR2010_01_14_T1_T2p5							x	
2.01	AAUDLR2010_02_01_T2_Rp1		x	x					
⋮	⋮		⋮	⋮					
2.09	AAUDLR2010_02_09_T2_Rp9		x	x					
2.10	AAUDLR2010_02_10_T2_T1p1							x	
⋮	⋮							⋮	
2.14	AAUDLR2010_02_14_T1_T1p5							x	
3.01	AAUDLR2010_03_01_T3_Rp1							x	
⋮	⋮							⋮	
3.9	AAUDLR2010_03_20_T3_Rp9							x	
3.10	AAUDLR2010_03_10_T3_T1p1							x	
⋮	⋮							⋮	
3.14	AAUDLR2010_03_14_T3_T1p5							x	
3.15	AAUDLR2010_03_15_T3_T2p1							x	
⋮	⋮							⋮	
3.19	AAUDLR2010_03_19_T3_T2p5							x	
3.20	AAUDLR2010_03_20_T3_Rp6								x
4.01	AAUDLR2010_04_01_T1_Rp1						x		
4.02	AAUDLR2010_04_02_T1_Rp2						x		
4.03	AAUDLR2010_04_03_T1_Rp3						x		
5.01	AAUDLR2010_05_01_T1_Rp4_win1				x				
⋮	⋮				⋮				
5.04	AAUDLR2010_05_04_T1_Rp4_win1234				x				
5.05	AAUDLR2010_05_05_T1_Rp1_win1				x				
⋮	⋮				⋮				
5.08	AAUDLR2010_05_08_T1_Rp1_win1234				x				
5.09	AAUDLR2010_05_09_T1_Rp2_win1				x				
⋮	⋮				⋮				
5.12	AAUDLR2010_05_12_T1_Rp2_win1234				x				
5.13	AAUDLR2010_05_13_T1_Rp3_win1				x				
⋮	⋮				⋮				
5.16	AAUDLR2010_05_16_T1_Rp3_win1234				x				
6.01	AAUDLR2010_06_01_T1_Rp3_win1to9					x			
6.02	AAUDLR2010_06_02_T1_Rp4_win1to9					x			
6.03	AAUDLR2010_06_03_T1_Rp2_win1to9					x			

Table 5.2: Noise Measurement for Experiment of Section 5.1.1 .

Scen. # 0.00	Tx Track	Rx Pos.	Comments	Calibration File (suffix ".KOR")	Filename (suffix ".000.DLR1_DSK")
0.00	T1	Rp4	[1]	AAUDLR2010_cal_01	AAUDLR2010_noise_01

Comments:

[1] 20 s were recorded with transmitter switched off.

5.5.2 Measurements of Scenario 1

The measurements of scenario 1 consist of all measurements with the transmitter on track T1 with the receiver positions Rp1 to Rp9 and the positions T2Rp1 to T2Rp5. The room was empty and all windows were closed. The measurement team was standing outside in the corridor during the measurement process. The measurements of scenario 1.01 to 1.09 correspond to the experiment described in Section 5.1.2. The measurements of scenario 1.09 to 1.14 are intended for co-operative localization experiments and correspond to the experiment described in Section 5.3.

Table 5.3: Measurements for Transmitter on Track T1.

Scen. #	Tx Track	Rx Pos.	Comments	Calibration File (suffix ".KOR")	Filename (suffix ".000.DLR1_DSK")
1.01	T1	Rp1		AAUDLR2010_cal_01	AAUDLR2010_01_01_T1_Rp1
1.02	T1	Rp2		AAUDLR2010_cal_01	AAUDLR2010_01_02_T1_Rp2
1.03	T1	Rp3	[4]	AAUDLR2010_cal_01	AAUDLR2010_01_03_T1_Rp3
1.04	T1	Rp4	[5]	AAUDLR2010_cal_01	AAUDLR2010_01_01_T1_Rp4
1.05	T1	Rp5	[1],[6]	AAUDLR2010_cal_03	AAUDLR2010_02_05_T1_Rp5
1.06	T1	Rp6	[2]	AAUDLR2010_cal_03	AAUDLR2010_01_06_T1_Rp6
1.07	T1	Rp7		AAUDLR2010_cal_03	AAUDLR2010_01_07_T1_Rp7
1.08	T1	Rp8		AAUDLR2010_cal_03	AAUDLR2010_01_08_T1_Rp8
1.09	T1	Rp9		AAUDLR2010_cal_01	AAUDLR2010_01_09_T1_Rp9
1.10	T1	T2p1		AAUDLR2010_cal_01	AAUDLR2010_01_10_T1_T2p1
1.11	T1	T2p2		AAUDLR2010_cal_01	AAUDLR2010_01_11_T1_T2p2
1.12	T1	T2p3		AAUDLR2010_cal_01	AAUDLR2010_01_12_T1_T2p3
1.13	T1	T2p4		AAUDLR2010_cal_01	AAUDLR2010_01_13_T1_T2p4
1.14	T1	T2p5		AAUDLR2010_cal_01	AAUDLR2010_01_14_T1_T2p5

Comments:

[1] All measurements with Rp5 were measured at the end of the Tx T1 and T2 measurements, because the Rx needed to be moved from tripod to the table.

[2] Was measured after all measurements in R4 with T1 and T2 were finished.

[3] Change of the Rx height from 110 cm to 120 cm.

[4] Plastic strips mounting the Rx antenna MUX loosened. It needed to be tightened again. New stronger plastic strips were used.

[5] Scenario 1.04 was saved with the wrong file name. Manual fix afterwards.

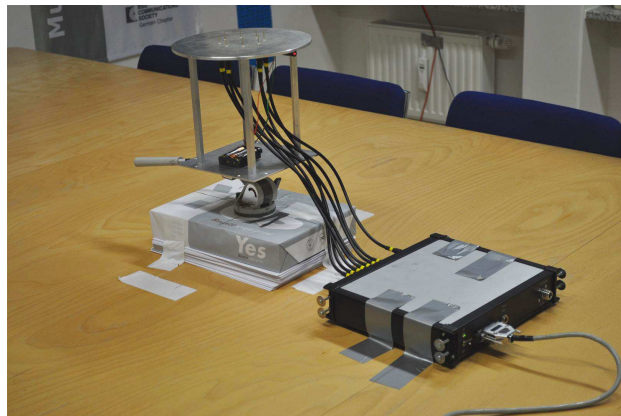[6] Scenario 1.05 was saved with the wrong filename. Manual fix afterwards.

Figure 5.1: Mounting of the Rx array and the multiplexer on the table for the receiver position Rp5.

5.5.3 Measurements of Scenario 2

The measurements of scenario 2 consist of all measurements with the transmitter on track T2 with the receiver positions Rp1 to Rp9 and the positions T1Rp1 to T1Rp5. The room was empty and all windows were closed. The measurement team was standing outside in the corridor during the measurement process. The measurements of scenario 2.01 to 2.09 correspond to the experiment described in Section 5.1.2. The measurements scenario 2.09 to 2.14 are intended for cooperative localization and are described in Section 5.3.

Table 5.4: Measurements for Transmitter on Track T2.

Scen. #	Tx Track	Rx Pos.	Comments	Calibration File (suffix ".KOR")	Filename (suffix ".000.DLR1_DSK")
2.01	T2	Rp1		AAUDLR2010_cal_02	AAUDLR2010_02_01_T2_Rp1
2.02	T2	Rp2		AAUDLR2010_cal_02	AAUDLR2010_02_02_T2_Rp2
2.03	T2	Rp3		AAUDLR2010_cal_02	AAUDLR2010_02_03_T2_Rp3
2.04	T2	Rp4		AAUDLR2010_cal_02	AAUDLR2010_02_04_T2_Rp4
2.05	T2	Rp5		AAUDLR2010_cal_03	AAUDLR2010_02_05_T2_Rp5
2.06	T2	Rp6		AAUDLR2010_cal_03	AAUDLR2010_02_06_T2_Rp6
2.07	T2	Rp7		AAUDLR2010_cal_03	AAUDLR2010_02_07_T2_Rp7
2.08	T2	Rp8		AAUDLR2010_cal_03	AAUDLR2010_02_08_T2_Rp8
2.09	T2	Rp9		AAUDLR2010_cal_02	AAUDLR2010_02_09_T2_Rp9
2.10	T2	T2p1		AAUDLR2010_cal_02	AAUDLR2010_02_10_T2_T1p1
2.11	T2	T2p2		AAUDLR2010_cal_02	AAUDLR2010_02_11_T2_T1p2
2.12	T2	T2p3		AAUDLR2010_cal_02	AAUDLR2010_02_12_T2_T1p3
2.13	T2	T2p4		AAUDLR2010_cal_02	AAUDLR2010_02_13_T2_T1p4
2.14	T2	T2p5		AAUDLR2010_cal_02	AAUDLR2010_02_14_T2_T1p5

Comments:

Track T2 is longer than T1. The measurement files are approximately 60 s long.
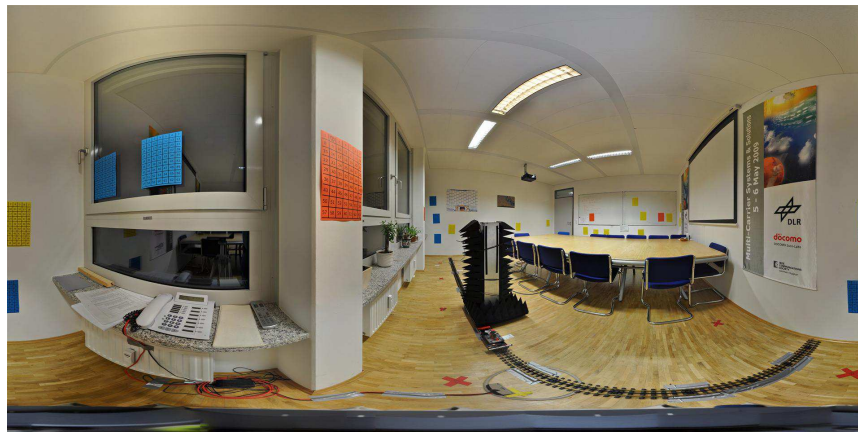

Figure 5.2: Panograph from Rp1 perspective showing track T2, the train and the antenna tower.

5.5.4 Measurements of Scenario 3

All measurements of scenario 3 are with the transmitter on track T3 with the receiver positions Rp1 to Rp9, T1Rp1 to T1Rp5 and the positions T2Rp1 to T2Rp5. The room was empty and all windows were closed. The measurement team was standing outside in the corridor during the measurement process. The measurements of scenario 3 are intended for cooperative localization and their purpose is described in Section 5.3.

Furthermore the measurement of scenario 3.20 was a measurement with the Tx standing at the end of track T3. In this measurement the lights (fluorescent tubes) were in the beginning switched of and after approximately 20 seconds switched on. This measurement corresponds to experiment 4.1 described in Section 5.4.1.

Table 5.5: Measurements for Transmitter on Track T3.

Scen. #	Tx Track	Rx Pos.	Comments	Calibration File (suffix ".KOR")	Filename (suffix ".000.DLR1_DSK")
3.01	T3	Rp1		AAUDLR2010_cal_05	AAUDLR2010_03_01_T3_Rp1
3.02	T3	Rp2		AAUDLR2010_cal_05	AAUDLR2010_03_02_T3_Rp2
3.03	T3	Rp3		AAUDLR2010_cal_05	AAUDLR2010_03_03_T3_Rp3
3.04	T3	Rp4		AAUDLR2010_cal_05	AAUDLR2010_03_04_T3_Rp4
3.05	T3	Rp5		AAUDLR2010_cal_04	AAUDLR2010_03_05_T3_Rp5
3.06	T3	Rp6		AAUDLR2010_cal_06	AAUDLR2010_03_06_T3_Rp6
3.07	T3	Rp7	[1]	AAUDLR2010_cal_06	AAUDLR2010_03_07_T3_Rp7
3.08	T3	Rp8		AAUDLR2010_cal_05	AAUDLR2010_03_08_T3_Rp8
3.09	T3	Rp9		AAUDLR2010_cal_05	AAUDLR2010_03_09_T3_Rp9
3.10	T3	T1p1		AAUDLR2010_cal_05	AAUDLR2010_03_10_T3_T1p1
3.11	T3	T1p2		AAUDLR2010_cal_05	AAUDLR2010_03_11_T3_T1p2
3.12	T3	T1p3		AAUDLR2010_cal_05	AAUDLR2010_03_12_T3_T1p3
3.13	T3	T1p4		AAUDLR2010_cal_05	AAUDLR2010_03_13_T3_T1p4
3.14	T3	T1p5		AAUDLR2010_cal_05	AAUDLR2010_03_14_T3_T1p5
3.15	T3	T2p1		AAUDLR2010_cal_05	AAUDLR2010_03_15_T3_T2p1
3.16	T3	T2p2		AAUDLR2010_cal_05	AAUDLR2010_03_16_T3_T2p2
3.17	T3	T2p3		AAUDLR2010_cal_05	AAUDLR2010_03_17_T3_T2p3
3.18	T3	T2p4		AAUDLR2010_cal_05	AAUDLR2010_03_18_T3_T2p4
3.19	T3	T2p5		AAUDLR2010_cal_05	AAUDLR2010_03_19_T3_T2p5
3.20	T3	Rp6	[2]	AAUDLR2010_cal_06	AAUDLR2010_03_20_T3_Rp6lights

Comments:
[1] Door to R2 was open.
[2] Measurement with the train at the end of the track. First 20 seconds lights switched off. After 20 seconds lights (flourescent tubes) switched on.

Figure 5.3: Panograph from Rp6 perspective showing the interior of room R3 and track T3.

5.5.5 Measurements of Scenario 4

The measurements of scenario 4 consist of all measurements with the transmitter on track T1 with the receiver positions Rp2 to Rp4. Around the meeting table were 10 people sitting (Fig. 5.4) and all windows were closed. The purpose of the measurements is described in Section 5.2.3.

Table 5.6: Measurements with 10 persons R4.

Scen. #	Tx Track	Rx Pos.	Comments	Calibration File (suffix ".KOR")	Filename (suffix ".000.DLR1_DSK")
4.01	T1	Rp1		AAUDLR2010_cal_02	AAUDLR2010_04_01_T1_Rp2
4.02	T1	Rp2		AAUDLR2010_cal_02	AAUDLR2010_04_02_T1_Rp3
4.03	T1	Rp3		AAUDLR2010_cal_02	AAUDLR2010_04_03_T1_Rp4

Comments:
10 people were sitting in the room around the table. People were asked to not move. No Laptops or any other additional equipment.

Figure 5.4: Ten persons placed around the meeting room table.

5.5.6 Measurements of Scenario 5

The measurements of scenario 5 consist of all measurements with the transmitter on track T1 with the receiver positions Rp1 to Rp4 and open windows. The purpose of the measurements is described in Section 5.2.1. The windows open to the inside (Fig. 5.5) and the frames of the windows are metallic. Notice at receiver position Rp1 is window number 4 and at Rp2 window number 1 above the receiver array when these windows are opened. An influence on the antenna response due to the metallic window frame is expected. The order of opening the windows at position Rp2 was changed as compared to the other measurements. The intention was that only when all 4 windows are open, window 1 is above Rp2.

Table 5.7: Measurements with open windows.

Scen. #	Tx Track	Rx Pos.	Comments	Calibration File (suffix ".KOR")	Filename (suffix ".000.DLR1_DSK")
5.01	T1	Rp4	[1]	AAUDLR1010_cal_02	AAUDLR2010_05_01_T1_Rp4_win1
5.02	T1	Rp4	[2]	AAUDLR1010_cal_02	AAUDLR2010_05_02_T1_Rp4_win12
5.03	T1	Rp4	[3]	AAUDLR1010_cal_02	AAUDLR2010_05_03_T1_Rp4_win123
5.04	T1	Rp4	[4]	AAUDLR1010_cal_02	AAUDLR2010_05_04_T1_Rp4_win1234
5.05	T1	Rp1	[1]	AAUDLR1010_cal_02	AAUDLR2010_05_05_T1_Rp1_win1
5.06	T1	Rp1	[2]	AAUDLR1010_cal_02	AAUDLR2010_05_06_T1_Rp1_win12
5.07	T1	Rp1	[3]	AAUDLR1010_cal_02	AAUDLR2010_05_07_T1_Rp1_win123
5.08	T1	Rp1	[4]	AAUDLR1010_cal_02	AAUDLR2010_05_08_T1_Rp1_win1234
5.09	T1	Rp2	[5]	AAUDLR1010_cal_02	AAUDLR2010_05_09_T1_Rp2_win4
5.10	T1	Rp2	[6]	AAUDLR1010_cal_02	AAUDLR2010_05_10_T1_Rp2_win34
5.11	T1	Rp2	[7]	AAUDLR1010_cal_02	AAUDLR2010_05_11_T1_Rp2_win234
5.12	T1	Rp2	[4]	AAUDLR1010_cal_02	AAUDLR2010_05_12_T1_Rp2_win1234
5.13	T1	Rp3	[1]	AAUDLR1010_cal_02	AAUDLR2010_05_13_T1_Rp3_win1
5.14	T1	Rp3	[2]	AAUDLR1010_cal_02	AAUDLR2010_05_14_T1_Rp3_win12
5.15	T1	Rp3	[3]	AAUDLR1010_cal_02	AAUDLR2010_05_15_T1_Rp3_win123
5.16	T1	Rp3	[4]	AAUDLR1010_cal_02	AAUDLR2010_05_16_T1_Rp3_win1234

Comments:
[1] W1 open.
[2] W1 and W2 open.
[3] W1, W2 and W3 open.
[4] W1, W2, W3 and W4 open.
[5] W4 open.
[6] W3 and W4 open.
[7] W2, W3 and W4 open.

(a)   (b)

Figure 5.5: (a) The receiver is at position Rp1 and W1 to W4 are open. (b) The receiver at position Rp2. The metallic frame of W1 is only approximatly 10 cm above the antenna array.

5.5.7 Measurements of Scenario 6

The measurements of scenario 6 consist of measurements with the transmitter on track T1 with the receiver positions Rp2 to Rp4. The windows W1 to W9 in the rooms R2, R3 and R4 were open during the measurements. The intended use of the measurements is described in Section 5.2.2.

Table 5.8: Measurements with window W1 to W9 open.

Scen. #	Tx Track	Rx Pos.	Comments	Calibration File (suffix ".KOR")	Filename (suffix ".000.DLR1_DSK")
6.01	T1	Rp3		AAUDLR2010_cal_02	AAUDLR2010_06_01_T1_Rp3_win1to9
6.02	T1	Rp4		AAUDLR2010_cal_02	AAUDLR2010_06_02_T1_Rp4_win1to9
6.03	T1	Rp2		AAUDLR2010_cal_02	AAUDLR2010_06_03_T1_Rp2_win1to9

Comments:
The windows in room R2, R3 and R4 were open.

CHAPTER 6

DATA STRUCTURE AND FILE NAMES

6.1 Import of RAW Measurement Data

The descriptions in the previous sections refer to the measurement data in the raw channel sounder format. In order to use this data format a 32 bit Matlab version is necessary to use the MEDAV import functions. DLR's MEDAV sounder uses an older file format which is not compatible with the currently distributed "Hyeff" filters from MEDAV. One can obtain with the "Hyeff" licence the import functions for the DLR sounder, directly from DLR.

6.1.1 Import Functions and Data Formats

In the following we state some example Matlab code to import the measurement data with the Medav functions.

```
[Error, Header] = RSKHead(0,[measurementFolder filename],0 );
[Error, Info] = RSKInfo(0,[measurementFolder filename],0 );
for iLoop=1:Header.DataSets
[Error, Data, Snap] = RSKData(0,[measurementFolder filename],...
        [(iLoop−1)∗Header.SetsPerFDBlock+1 1 iLoop∗Header.SetsPerFDBlock],...
        [257 1 1793], [1 2 3 4 5 6 7 8], [],[],0,[],0 );
[Error, Nav, GPS] = RSKNav(0,[measurementFolder filename],...
        [(iLoop−1)∗Header.SetsPerFDBlock+1:1:iLoop∗Header.SetsPerFDBlock],0 );
end
```

The code above imports in every iteration one burst of data with the `RSKData()` function. The function uses a vector specifying the measurement cycles to import. We specify this vector in Matlab as
`[(iLoop-1)*Header.SetsPerFDBlock+1 1 iLoop*Header.SetsPerFDBlock]`
to import all cycles with the burst index `iLoop`. In the raw data file and for the used measurement settings consists each measured frequency response of 2048 samples from which only a part is non zero. We obtain the non zero part with the vector `[257 1 1793]`, which specifies the first frequency sample (257), the step size in

Table 6.1: Data fields of the "Header" structure.

Fieldname	Value
DataSets	7140
Channels	8
FDDChannels	1
MeasureMode	2
MeasureModeText	'Time grid mode'
FDDMode	0
FDDModeText	'FDD disabled'
Periode	2048
TxCount	1
Grid	131.0720
Bandwidth	120000000
RF	5.2000e+009
FDD-RF	[250000000 250000000]
IF	80000000
SampleFreq	320000000
FDBlocksPerDBlock	1
SetsPerFDBlock	20
PreProcessing	1
PreProcessingText	'Rowdata whithout preprocessing'
OdometerPulses	100000
NavDataSource	0
NavDataSourceText	'Receiver unit'
CalibTxPower	0
CalibAGC	87
CalibAttenuation	33
CalibFactor	0
MeasTxPower	0

samples (1) and the last sample (1793) out of the 2048. The measured receive antennas are selected with the vector [1 2 3 4 5 6 7 8]. The size of the "Data" variable is $N_{\text{burst}} \times N_{\text{c}} \times N_{\text{Rx}}$ ($20 \times 1537 \times 8$). For a detailed overview of the function description we refer to the headers in the source code of the import functions. The fields of the other data structures are listed in Table 6.1, Table 6.2, and Table 6.3.

6.2 Detection of Erroneous Frequency Responses

Using long cables to the antenna multiplexer creates random distortions in the measured frequency responses. The frequency responses with such distortions need to be detected automatically such that one can decide to include these data or not. We observe these distortions as a drop in the power of the frequency response for some arbitrary frequency ranges. The size of these frequency ranges and their locations in the considered bandwidth is random over the different measured frequency responses.

During our measurements were no moving objects in the room and the transmitter moved only 0.0035λ during one burst. Thus we assume that the measured frequency responses of N_{burst} is constant at each antenna. In order to detect the frequency distortions from the antenna multiplexer we compare each measured frequency response to an averaged frequency response. We represent the measured frequency response as $H_{i,j}(f)$ where $j = 1 \ldots N_{\text{Rx}}$ is the index for the number of receive antennas and $i = 1 \ldots N_{\text{burst}}$ is the index of the cycles in a burst. We calculate

Table 6.2: Data fields of the "Info" structure.

Fieldname	Value
MeasFileName	'D:\RUSKData\Data\WHERE2_01_01_T1_Rp1.000.DLR1_DISK'
CalibFileName	'D:\RUSKData\Calibration\Where2_cal_01KOR'
StartTime	'02.01.1999; 04:28:10'
EndTime	'02.01.1999; 04:28:59'
MeasPlace	''
MeasSeries	''
MeasLeader	''
TxUnit	''
TxAntenna	'RUSK DLR 1.51 GHz 1x1-Tx-antenna (Id=1050, SNr. 24547)'
TxPosition	''
RxUnit	''
RxAntenna	'RUSK DLR external multiplexer 8 times, f=1..5.3GHz, Pmax=2W, Serial number 33563, Id=9050'
RxPosition	''
Comment1	''
Comment2	''
Comment3	''
Comment4	''
Comment5	''
Scenario	[49x1 struct]

Table 6.3: Data fields of the "Nav" structure.

Fieldname	Value
Number	[1 2 3 4 5 6 7 8 9 10 11 12 13 14 15 16 17 18 19 20]
RelTime	[0 0 0 0 0 0 0 0 0 0 0 0 0 0 0 0 0 0 0 0]
Time	[0 0 0 0 0 0 0 0 0 0 0 0 0 0 0 0 0 0 0 0]
Distance1	[1x20 double]
Distance2	[0 0 0 0 0 0 0 0 0 0 0 0 0 0 0 0 0 0 0 0]

the average frequency response for the j antenna in a burst as

$$\widehat{H}_j(f) = \frac{1}{N_{\text{burst}}} \sum_{i=1}^{N_{\text{burst}}} H_{i,j}(f). \tag{6.1}$$

We use these averaged frequency responses for each antenna to calculate the error between the averaged frequency responses and the frequency responses of each cycle in the burst as

$$\widehat{e}_{i,j}(f) = H_{i,j}(f) - \widehat{H}_j(f). \tag{6.2}$$

Furthermore we estimate the sample based standard deviation of the absolute values of the error over the measurement bandwidth as

$$\widehat{\sigma}_{i,j} = \sqrt{\frac{1}{N_c} \sum_f \left(|\widehat{e}_{i,j}(f)| - \frac{1}{N_c} \sum_f |\widehat{e}_{i,j}(f)| \right)^2}. \tag{6.3}$$

For the case the frequency responses of one antenna in a burst are not distorted, varies the standard deviation of the errors only due to measurement noise. If a distortion of a frequency response occurred is the standard deviation of the errors larger. We chose a threshold to detect distorted frequency responses. The threshold is calculated as the product of some constant value q and the minimum standard deviation of the error in a burst for each antenna. Thus we achieve the index set

$D_{i,j}$ of distorted frequency responses as

$$D_{i,j} = \mathbb{1}(\widehat{\sigma}_{i,j} > q \min_i \widehat{\sigma}_{i,j}), \tag{6.4}$$

where $\mathbb{1}$ is the indicator function. We obtain for each burst such an index $D_{i,j}$ set.

6.3   Measurement Data in Matlab Format

The mentioned import functions in Section 6.1 for the channel sounder data only work in specific 32 bit Matlab versions running on Windows. In order to allow for the use of the measurement data in 64 bit Matlab versions and on Linux systems are the data files converted in Matlab data files. The filenames are the same as the raw data files except that the suffix ".000.DLR1_DSK" is replaced by the file ending ".mat".

The data contained in these files are the "Header" and "Info" structures. In addition are the frequency responses of each burst stored in their own variable (eg. "Data0000001",…,"Data0001000"). This allows for easy access to specific bursts and not opening the complete data at once, which would results in huge memory consumption. Additionally are to each burst the indices of the detected distorted frequency responses saved. For the threshold we chose the value $q = 1.2$, based on some experimental tests. These indices are stored as logical variables and denoted eg. "IndexGood0000001" or "IndexBad0000001" for the good and bad indices of burst one. Similarly, for each burst are the "Gps" and "Nav" structures stored with the corresponding indices, eg. as"Gps0000001" and "Nav0000001".

BIBLIOGRAPHY

[1] Huber+Suhner, "Datasheet for Sencity Antenna For In-Carriage Wireless Communication, Type: SOA 5600/360/3/20/V_1," Document No. 01.02.1358, May 2007.

[2] S. McHugh, "Panoramic Image Projections," Online.

[3] A. Hamblenne and M. Therer, "The grid, Method for a precise location of the entrance pupil on a DLSR camera," PDF Online, Sept. 2004.